



# HHS Public Access

Author manuscript

*Angew Chem Int Ed Engl.* Author manuscript; available in PMC 2017 September 19.

Published in final edited form as:

*Angew Chem Int Ed Engl.* 2016 September 19; 55(39): 11770–11774. doi:10.1002/anie.201603844.

## Simultaneous Identification of Spectral Properties and Sizes of multiple Particles in Solution with sub-nm Size Resolution

Engin Karabudak<sup>1,2</sup>, Emre Brookes<sup>3</sup>, Vladimir Lesnyak<sup>4</sup>, Nikolai Gaponik<sup>4</sup>, Alexander Eychmüller<sup>4</sup>, Johannes Walter<sup>5,6</sup>, Doris Segets<sup>5,6</sup>, Wolfgang Peukert<sup>5,6</sup>, Wendel Wohlleben<sup>7</sup>, Borries Demeler<sup>3,\*</sup>, and Helmut Cölfen<sup>1,8,\*</sup>

<sup>1</sup>Max Planck Institute of Colloids and Interfaces, Colloid Chemistry, Research Campus Golm, Am Mühlenberg, D-14424 Potsdam, Germany

<sup>2</sup>Izmir Institute of Technology, Chemistry Department, TR-35430 Izmir, Turkey

<sup>3</sup>University of Texas Health Science Center at San Antonio, 7703 Floyd Curl Drive, San Antonio, TX 78229-3901, USA

<sup>4</sup>Physical Chemistry, TU Dresden, Bergstr. 66b, D-01062 Dresden, Germany

<sup>5</sup>Institute of Particle Technology (LFG), Friedrich-Alexander Universität Erlangen-Nürnberg (FAU), Cauerstr. 4, 91058 Erlangen, Germany

<sup>6</sup>Interdisciplinary Center for Functional Particle Systems (FPS), Friedrich-Alexander-Universität Erlangen-Nürnberg (FAU), Haberstr. 9a, 91058 Erlangen, Germany

<sup>7</sup>BASF SE, GKC/O - G201, 67056 Ludwigshafen, Germany

### Abstract

We report on an unsurpassed solution characterization technique based on analytical ultracentrifugation, which demonstrates exceptional potential for resolving particle size in solution with sub-nm resolution. We achieve this improvement in resolution by simultaneously measuring UV-Vis spectra while hydrodynamically separating individual components in the mixture. By equipping an analytical ultracentrifuge with a novel multi-wavelength detector, we are effectively adding a new spectral discovery dimension to traditional hydrodynamic characterization, and amplify the information learned by orders of magnitude. We demonstrate the power of this technique by characterizing unpurified CdTe nanoparticle samples, avoiding tedious and often impossible purification and fractionation of nanoparticles into apparently monodisperse fractions. By using our approach, we have for the first time identified the *pure* spectral properties and bandgap positions of *discrete* species present in the CdTe mixture.

---

Many small nanoparticles have size dependent optical properties due to effects like quantum confinement<sup>[1]</sup> or surface plasmon resonance.<sup>[2]</sup> Thus, these particles are highly promising

---

Correspondence and requests for materials should be addressed to H.C. (helmut.coelfen@uni-konstanz.de) or B.D. (demeler@biochem.uthscsa.edu).

<sup>8</sup>Present Address: University of Konstanz, Physical Chemistry, Universitätsstraße 10, D-78457 Konstanz, Germany

**Author Information** The authors declare no competing financial interests.

Supplementary Materials Figs. SI 1 - SI 9, Tab. SI 1 and SI 2 and Movies for Figs. 1 & 2.

for many optical, (opto)electronic, diagnostic, chemical or biomedical applications, since the particle properties can be tuned to optimize the physical and chemical performance.<sup>[3]</sup> Detailed knowledge of size, shape, molecular weight, and composition of these nanoparticles is required to understand their physical and chemical properties. So far, no experimental method has been able to comprehensively and accurately characterize these essential properties for polydisperse nanoparticles directly in solution. Here we show that analytical ultracentrifugation with a multi-wavelength detector coupled with 2-dimensional spectrum analysis can be used to resolve colloidal CdTe QDs with Angstrom resolution and with unrivaled statistical significance. The 30 minutes experiment, using only a few micrograms of the material revealed size, anisotropy, molar mass and partial concentration of 24 distinct CdTe QD species in a polydisperse mixture. We were able to determine underlying absorbance spectra and band gaps for the seven smallest monodisperse species in the mixture. This permits direct determination of the particle size dependence of the optical band gap in a single experiment. This example shows that our method is a general and reliable approach for the simultaneous high-resolution hydrodynamic and spectral characterization of any mixture containing size and spectral diversity. This intriguing combination is encountered in a wide range of fields, by far not limited to nanomaterials including quantum dots, metal nanoparticles or carbon nanotubes.

Analytical ultracentrifugation (AUC) is a classical method for colloid and polymer analysis and is particularly well suited for highly accurate size determination of nanoparticles suspended in solution.<sup>[4-5]</sup> During an AUC experiment particles are separated hydrodynamically in a centrifugal field based on their different size, mass, density and frictional properties, whereby the process of sedimentation is captured by different detectors such as absorbance, interference or fluorescence optics. The resulting sedimentation data are then evaluated to give access to the particle size distribution (PSD). Attempts to determine size-dependent spectral changes of QDs by fractionation of nanoparticle mixtures using a conventional single-wavelength detector have been reported.<sup>[6-7]</sup> However, due to the huge variability in spectral properties of slightly different QD species these measurements were severely limited in resolution and quality. Breakthroughs in both AUC hardware and data analysis software were necessary to advance this field of research. Recently, the resolution of AUC experiments has been significantly increased by applying more powerful techniques for data evaluation.<sup>[8-10]</sup> By means of this, size and shape distributions of various nanoparticles have been recently reported with high resolution.<sup>[11-12]</sup> However, due to single-wavelength detection, correlations between size and optical properties could not be resolved. In enhancing these measurements, we developed a unique multi-wavelength detector for AUC (MWL).<sup>[13-14]</sup> This detector allows for the determination of sedimentation profiles with a full visible spectrum for each radial point instead of only a single wavelength as in conventional instruments. Already the MWL raw data contain important information.<sup>[15-17]</sup> Recently, MWL has further been improved by a new data acquisition software and an enhanced detector setup.<sup>[18]</sup> However, to exploit the full potential of MWL and to access qualitative and quantitative properties of individual components in complex mixtures, the technique was coupled in this work with advanced evaluation available in the 2-dimensional spectrum analysis (2DSA).<sup>[10]</sup>

Starting with a heterogeneous mixture, 2DSA resolves individual species that are characterized by their anisotropy and molar mass (provided the particle density and hydration are known), hydrodynamic size, sedimentation and diffusion coefficients as well as partial concentration. 2DSA allows for high-resolution hydrodynamic analysis of MWL data, while simultaneously measuring the spectral properties of each species.

After acquiring individual absorbance spectra, eight CdTe fractions taken at appropriate time points during QD growth were mixed and subjected to band sedimentation in an ultracentrifuge equipped with a custom-built multi-wavelength detector.<sup>[13–14, 18]</sup> Over 36 minutes 20 scans of a wavelength range between 350 and 650 nm were recorded at 50 krpm and 25 °C. These eight quite narrow fractions yielded a blend with a broad size range. Figure 1 and Figure SI-1 show the experimental design and an example of the raw data from the MWL measurement as well as the evaluation method.

The resulting data were analyzed by 2DSA adapted for MWL. For each identified species, the CdTe core diameter, molar mass and individual wavelength spectra were extracted. The results of the data analysis are shown in Figure 2. The frictional ratio determined by 2DSA for all species suggested a spherical particle shape (Figure 2a), in agreement with electron microscopy results (Figure SI-2). The hydrodynamic separation resolved 24 species (Figure 2b and Table SI-1 for numerical data) from a mixture that was expected to contain only eight species. Smaller (< 4 nm) species isolated within the AUC run by 2DSA showed well-defined absorbance spectra (Figure 2c), clearly displaying a red shift of the absorption maximum with increasing particle size (Figure 2d).

The absorption profiles of Figure 2c are remarkably narrow with an unprecedented low absorption coefficient above the bandgap transition (well resolved for the two smallest species). Importantly, the particle sizes determined independently by 2DSA at each wavelength were consistent for all wavelengths from 350 to 650 nm. Integration over all species and wavelengths yielded the absorbance spectrum of the initial sample. This illustrates that 2DSA is a robust approach for analyzing sedimentation and diffusion distributions of nanoparticles from MWL experiments. The particle size resolution derived from the hydrodynamic calculations is very high, with a baseline resolution of about 1 Å for the smallest, and about 4 Å for the largest detected particles (Figure 2b). These calculations take into account that the density of stabilized nanoparticles gradually approaches the bulk density for larger CdTe core diameters due to the decreasing shell contribution from the hydrated thioglycolic acid stabilizer with associated solvent (Figure SI-3 and *Methods* section).<sup>[19]</sup> Changes in the shell morphology (thickness, density) can affect the resolution with respect to the core size. However, calculations showed that a variation of the shell thickness by 50 % does not alter the calculated core diameter by more than 1 Å. Therefore, resolution is not significantly affected by inhomogeneity of the shell. Further information on these error calculations are provided in the SI, Figure SI-4.

Independent from AUC, the particle size range and the fulfilled mass balance were confirmed. UV-Vis spectra of individual fractions shown in Figure 1a were deconvoluted to PSDs as described in Segets et al.<sup>[20]</sup> (*Methods* section) and weighted by their known

relative mixing ratios. The obtained dataset shows excellent agreement with the distribution derived from the absorbance data of the mixture shown in Figure 1b (Figure 3).

The latter verifies further the particle size range from AUC although the size resolution is expectedly much lower (Figure 2b) proving the validity of the density model in the AUC evaluation.

For the seven smallest nanoparticle sizes determined by 2DSA, we extracted the absorption maximum corresponding to the 1s-1s transition. These values (Figure 4) were compared to experimental [22] and calculated [21–22] literature data. Our values fit the theoretical curve for CdTe much better than data points obtained from conventional TEM imaging.[22]

Calculation of average particle sizes from the raw spectra allows to distinguish size steps less than 1 Å (Figure SI-5). From one single MW-AUC experiment and a simple core-shell assumption, not only (i) quasi monodisperse species with Å-resolution are isolated and (ii) unambiguously linked to their optical properties but also (iii) material properties are accessible without the need for calibration against another independent measurement technique.[20] In particular, the dependency of the band gap on the particle size can be measured in one single experiment.

Conversion of the 2DSA sedimentation coefficient distribution to the molar mass of each of the 24 discrete species is shown in Figure 5 (see Table SI-1 for detailed results).

Closer analysis reveals that the molecular weight of the smallest species is in agreement with the molecular weight predicted for a magic cluster of CdTe  $[\text{Cd}_{54}\text{Te}_{32}(\text{CH}_3\text{CH}_2\text{SH})_{52}]^{8-}$ . [21–23] To further demonstrate the resolution of MW-AUC, we investigated a single “monodisperse” [22, 24–25] CdTe fraction and observed two additional discrete species (Figure SI-6) corresponding to species observed in the mixture. Our results indicate that the present synthesis techniques are inadequate for generating truly monodisperse nanoparticles. Thus, previously reported UV/Vis spectra of CdTe nanoparticles [22, 24–25] are in fact a superposition of spectra of several species (Figure SI-7). Indeed, the UV/Vis spectrum of any CdTe nanoparticle sample can be successfully deconvoluted into the basis spectra from Figure 2, [26] and reveal the concentrations of truly monodisperse species present in the mixture (Figure SI-8). Noteworthy, MWL-AUC is the only technique that gives access to the latter.

In summary, we have developed a technique superior to any existing alternative that can simultaneously determine - in one single experiment - multimodal size distributions with Angström resolution, the absorbance spectrum and the respective band gap-size dependency, in a mixture of polydisperse CdTe nanoparticles directly in solution. Our data was validated simultaneously by hydrodynamic and spectral observations. The technique is adaptable to any of the many nanoparticle systems with size-dependent optical properties. Because MWL permits analysis of a large particle number (~1010), the resulting statistical confidence is much higher than time consuming conventional TEM measurements, where only a small number of particles is examined, which are subject to drying artifacts and aggregation. AUC has few solvent restrictions, needs only a few µg of sample and does not require sample purification. The method is especially effective for samples polydisperse in hydrodynamic

and spectral properties, and is thus valuable for any nanoparticle system as true monodispersity cannot be reached neither by synthesis nor fractionation. Our new approach will be of significant utility in the characterization of new semiconductor and metal nanoparticle systems directly after synthesis and without the need for purification. Furthermore, it can become a major tool for revealing nucleation and growth mechanisms with Angström particle size resolution in solution.<sup>[27]</sup>

## Supplementary Material

Refer to Web version on PubMed Central for supplementary material.

## Acknowledgments

We acknowledge the Max-Planck society as well as BASF SE, Ludwigshafen for financial support of this project. The development of the data analysis methods was supported by the National Institutes of Health Grant RR022200 (B.D.) and NSF ACI-1339649 (B.D.), and supercomputer time on XSEDE resources at the Texas Advanced Computing Center was provided by National Science Foundation grant TG-MCB070039N (B.D.). J.W. and W.P. acknowledge financial support of DFG through project "PE 427/28-1" and the Erlangen Cluster of Excellence "Engineering of Advanced Materials".

## References

1. Alivisatos AP. *Science*. 1996; 271:933–937.
2. El-Sayed MA. *Accounts of Chemical Research*. 2001; 34:257–264. [PubMed: 11308299]
3. Talapin DV, Lee JS, Kovalenko MV, Shevchenko EV. *Chemical Reviews*. 2010; 110:389–458. [PubMed: 19958036]
4. Cölfen H, Pauck T. *Colloid and Polymer Science*. 1997; 275:175–180.
5. Cölfen H, Schnablegger H, Fischer A, Jentoft FC, Weinberg G, Schlögl R. *Langmuir*. 2002; 18:3500–3509.
6. Cölfen H, Pauck T, Antonietti M. *Progress in Colloid and Polymer Science, Analytical Ultracentrifugation IV*. 1997; 107:136–147.
7. Niederberger M, Garnweitner G, Krumeich F, Nesper R, Cölfen H, Antonietti M. *Chemistry of Materials*. 2004; 16:1202–1208.
8. Demeler B, Tich-Lam N, Gorbet GE, Schirf V, Brookes EH, Mulvaney P, El-Ballouli AaO, Pan J, Bakr OM, Demeler AK, Uribe BIH, Bhattarai N, Whetten RL. *Analytical Chemistry*. 2014; 86:7688–7695. [PubMed: 25010012]
9. Gorbet G, Devlin T, Uribe BIH, Demeler AK, Lindsey ZL, Ganji S, Breton S, Weise-Cross L, Lafer EM, Brookes EH, Demeler B. *Biophysical Journal*. 2014; 106:1741–1750. [PubMed: 24739173]
10. Brookes E, Cao W, Demeler B. *European Biophysics Journal*. 2010; 39:405–414. [PubMed: 19247646]
11. Carney RP, Kim JY, Qian HF, Jin RC, Mehenni H, Stellacci F, Bakr OM. *Nature Communications*. 2011; 2
12. Nontapot K, Rastogi V, Fagan JA, Reipa V. *Nanotechnology*. 2013; 24
13. Bhattacharyya SK, Maciejewska P, Börger L, Stadler M, Gülsun AM, Cicek HB, Cölfen H. *Progress in Colloid and Polymer Science, Analytical Ultracentrifugation VIII*. 2006; 131:9–22.
14. Strauss HM, Karabudak E, Bhattacharyya S, Kretzschmar A, Wohlleben W, Cölfen H. *Colloid and Polymer Science*. 2008; 286:121–128. [PubMed: 19816525]
15. Pearson JZ, Krause F, Haffke D, Demeler B, Schilling K, Colfen H. *Methods in enzymology*. 2015; 562
16. Karabudak E, Wohlleben W, Cölfen H. *European Biophysics Journal*. 2010; 39:397–403. [PubMed: 19242689]

17. Backes C, Karabudak E, Schmidt CD, Hauke F, Hirsch A, Wohlleben W. *Chemistry-a European Journal*. 2010; 16:13176–13184.
18. Walter J, Loehr K, Karabudak E, Reis W, Mikhael J, Peukert W, Wohlleben W, Coelfen H. *Acs Nano*. 2014; 8:8871–8886. [PubMed: 25130765]
19. Jamison JA, Krueger KM, Yavuz CT, Mayo JT, LeCrone D, Redden JJ, Colvin VL. *ACS Nano*. 2008; 2:311–319. [PubMed: 19206632]
20. Segets D, Gradl J, Taylor RK, Vassilev V, Peukert W. *Acs Nano*. 2009; 3:1703–1710. [PubMed: 19507865]
21. Rogach AL, Katsikas L, Kornowski A, Su DS, Eychmuller A, Weller H. *Berichte Der Bunsen-Gesellschaft-Physical Chemistry Chemical Physics*. 1996; 100:1772–1778.
22. Rogach AL, Franzl T, Klar TA, Feldmann J, Gaponik N, Lesnyak V, Shavel A, Eychmüller A, Rakovich YP, Donegan JF. *Journal of Physical Chemistry C*. 2007; 111:14628–14637.
23. Rockenberger J, Troger L, Rogach AL, Tischer M, Grundmann M, Eychmuller A, Weller H. *Journal of Chemical Physics*. 1998; 108:7807–7815.
24. Murray CB, Norris DJ, Bawendi MG. *Journal of the American Chemical Society*. 1993; 115:8706–8715.
25. Yu WW, Qu LH, Guo WZ, Peng XG. *Chemistry of Materials*. 2003; 15:2854–2860.
26. Demeler, B.; Gorbet, G. *Analytical Ultracentrifugation Data Analysis with UltraScan-III*, Ch. 8 in *Analytical Ultracentrifugation: Instrumentation, Software, and Applications*. Uchiyama, S.; Stafford, WF.; Laue, T., editors. Springer; 2016.
27. Völkle CM, Gebauer D, Cölfen H. *Faraday Discussions*. 2015; 179:59–77. [PubMed: 25871922]

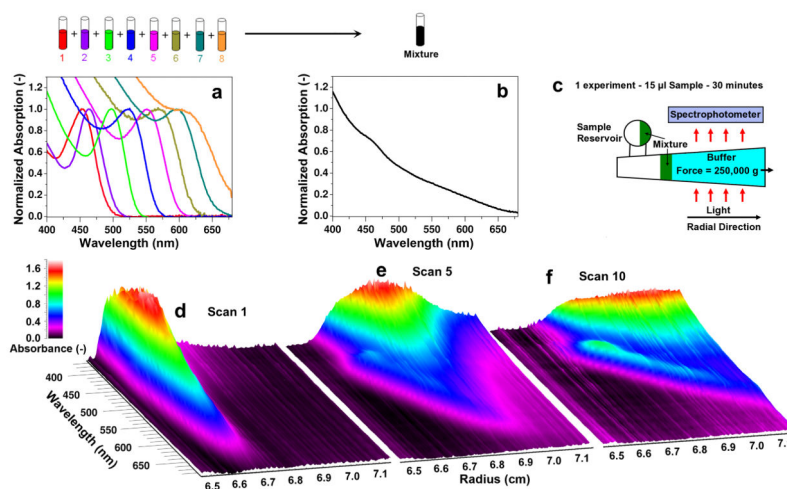


**Figure 1.**

(a) Eight different CdTe QD colloids were synthesized and absorbance spectra for all samples were acquired. (b) Particles were then mixed and the superimposed absorbance spectrum was obtained. (c) 15  $\mu\text{l}$  of the mixture was subjected to a band sedimentation experiment, and 20 sedimentation scans were acquired by MWL (three scans from the beginning, middle and end of this experiment are shown in d–f). The red shift of absorption with increasing particle size is clearly visible in the experimental data, where the sedimenting boundary is found at increasingly higher radial positions (corresponding to larger particles with faster sedimentation rate) and longer wavelengths. A video sequence (“Sedimentation Movie”) of the experiment is included in the supporting information (SI).

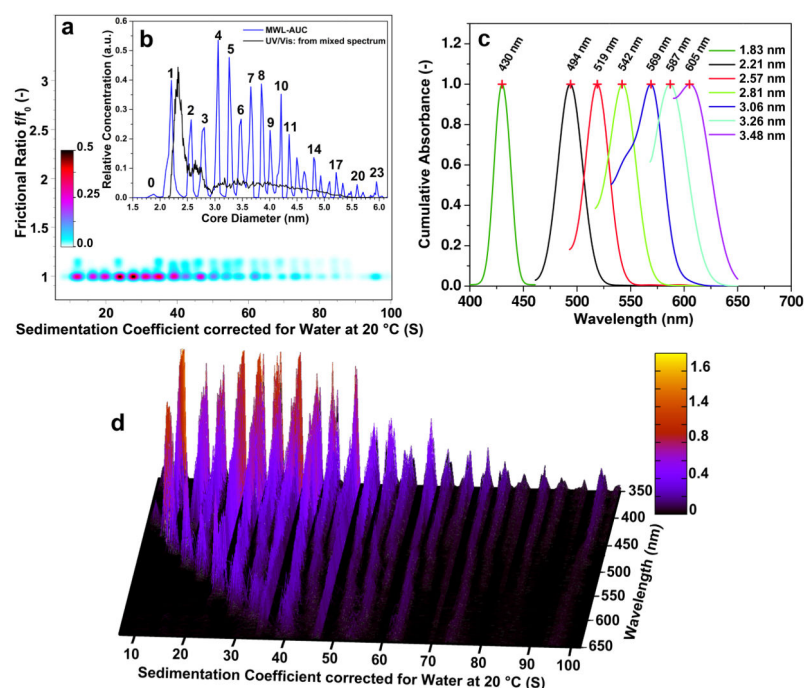


**Figure 2.**

(a) 2DSA for the mixture of nanoparticles shown in Figure 1, integrated over all analyzed wavelengths. Darker color indicates higher relative concentration. A frictional ratio of 1.0 indicates a spherical structure. (b) Concentration histogram transformation of the sedimentation coefficient to particle core diameter (without ligand/solvation shell) for the data shown in (a) together with the results of the core distribution evaluated by deconvolution of the mixture absorption shown in Figure 1b. Each peak represents the integrated concentrations from all wavelengths. Each species is labeled with a number, the zeroth species denotes the magic cluster. (c) The 1s-1s transition maxima from the absorbance spectra of the first 7 species isolated during the AUC experiment with the corresponding CdTe core diameters (legend on right). (d) Partial concentration of each species in optical density units plotted over sedimentation coefficient and absorption wavelength. 2DSA analysis resulted in a clear baseline separation of 24 individual species, consistently reproduced for all wavelengths (see “2DSA movie” video sequence in SI).



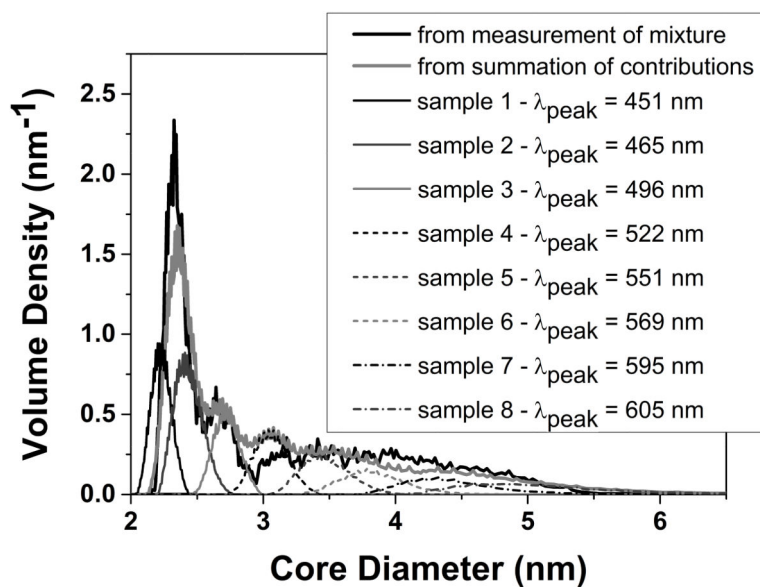


**Figure 3.** Particle size distribution (PSD) derived from the absorption data of the mixture (Figure 1b) together with the PSDs of the isolated fractions 1 (red – peak at 451 nm), 2 (violet – peak at 465 nm), 3 (green – peak at 496 nm), 4 (blue – peak at 522 nm), 5 (pink – peak at 551 nm), 6 (dark yellow – peak at 569 nm), 7 (cyan – peak at 595 nm) and 8 (orange – peak at 605 nm) (Figure 1), weighed by their mass contributions in the mixture as given in Table SI-2. The grey line is the summation of contributions 1–8 and evidences the nearly closed mass balance.

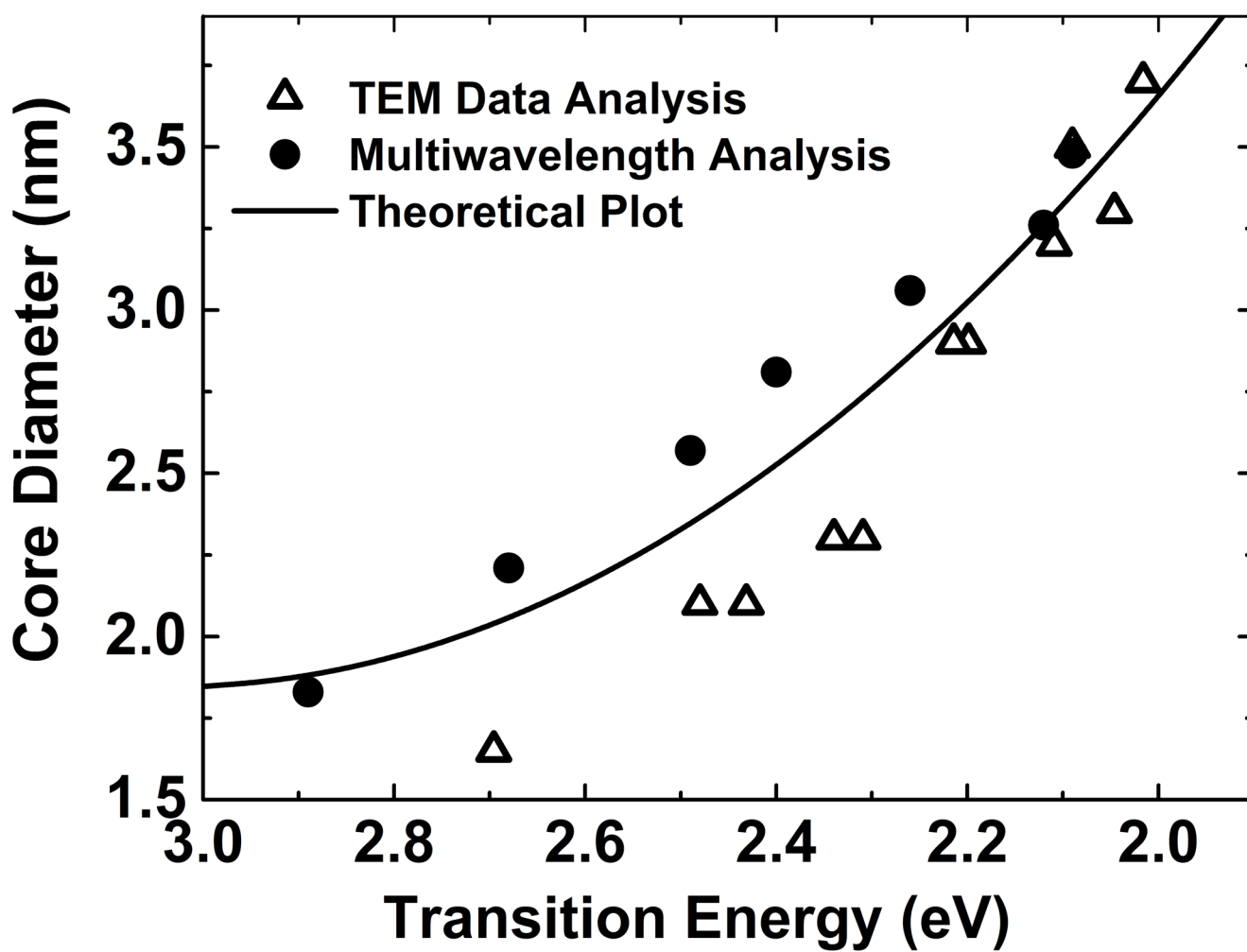


**Figure 4.** Size-absorption relation from a single MW-AUC measurement (filled circles): Comparison with theory<sup>[21]</sup> (solid line) and results from TEM analysis (open triangles) of purified samples.<sup>[22]</sup>

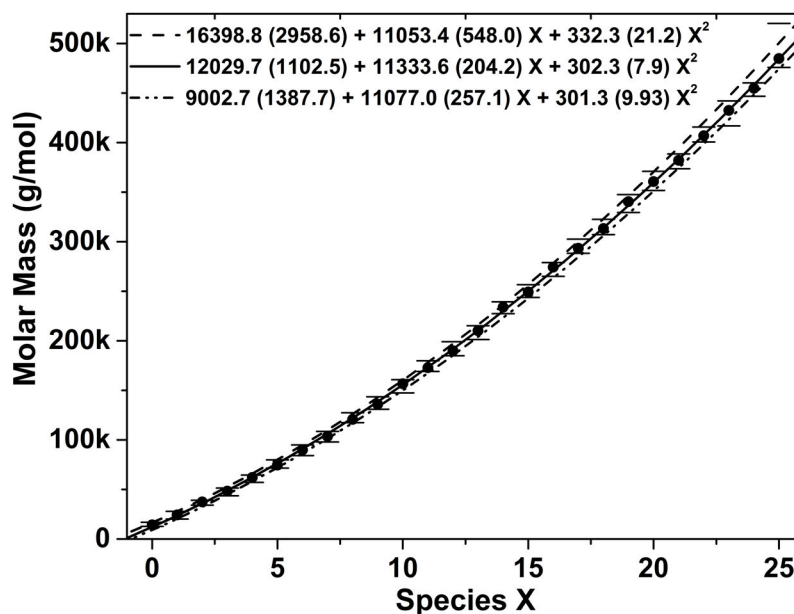


**Figure 5.**

Molar mass determined for the species identified in a 25-iteration 2-dimensional spectrum analysis (2DSA) Monte Carlo analysis. The mean and 95% confidence interval data fit well to a second-order polynomial and suggest a molar mass of 12,030 (+4,370/−3,027) g/mol for the smallest species (center: solid line, positive confidence band: dashed line, negative confidence band: dash-dotted line, formulas for the 2<sup>nd</sup> order polynomial are shown in the graph, including the standard errors in parenthesis, 95% confidence interval limits for individual measurements are shown as horizontal bars). This fit suggests that the molecular weight difference between individual species is equal to the smallest species observed, which is in good agreement with the molecular weight predicted for the magic cluster of CdTe  $[\text{Cd}_{54}\text{Te}_{32}(\text{CH}_3\text{CH}_2\text{SH})_{52}]^{8-}$  with a core diameter of 1.8 nm.<sup>[23]</sup>